

EXPERIMENTAL STUDY OF THE FLEXURAL STRENGTH AND DUCTILITY OF POST BURNED STEEL FIBER RC BEAMS

Antonius^{1*}, Purwanto², Primasiwi Harprastanti²

¹*Department of Civil Engineering, Faculty of Engineering, Universitas Islam Sultan Agung, Semarang 50112, Indonesia*

²*Department of Civil Engineering, Faculty of Engineering, Universitas Diponegoro, Jl. Prof. Soedarto, SH Tembalang, Semarang 50275, Indonesia*

(Received: June 2018 / Revised: July 2018 / Accepted: October 2018)

ABSTRACT

This paper presents an experimental study of eight reinforced concrete beams and aims to evaluate the flexural behavior and ductility of burned beams at various temperatures. The beam specimens contained steel fibers comprising 0.5% of the volume of the concrete. They were divided into two types, with the flexural region consisting of a single reinforcement system (without compressive reinforcement) and double reinforcement bars. Each type of beam was controlled (not burned), and burned at 300°C, 600°C and 900°C. The beam testing employed a four-point loading system (pure bending in the test region) and worked monotonically. The experimental results show that the performance of beams with the double reinforcement system to the resilient load was better than with a single reinforcement system beam. This occurred at normal temperatures and up to high temperatures. The longitudinal reinforcement installed inside the beam was very well protected and only lost yield stress of 17% of the initial stress, even though the beam was burned at high temperatures. The analysis of the flexural beam capacity using the stress-strain model of steel fibers at elevated temperatures shows that the results differed little from the flexural capacity of the experimental results.

Keywords: Beam; Ductility; Flexure strength; Steel fiber; Temperatures

1. INTRODUCTION

Steel fibrous concrete has been a popular material for more than three decades because of its excellent mechanical properties, such as shrinkage and a relatively low creep, high toughness and non-corrosive nature. The inter-conjugated matrix bonds in steel-reinforced concrete play a major role in maintaining the compactness of the constituents, so the steel-fiber concrete has excellent cracking strength (Jansson et al., 2012; Iqbal et al., 2015; Dhinakaran et al., 2016; Janani & Santhi, 2018). Steel fibers also play an important role in significantly increasing the ductility of concrete (Antonius, 2015; Han et al., 2015). Therefore, this material has high energy absorption properties compared to normal concrete, so it is useful when used as a structural material for earthquake resistance. However, steel fibrous concrete has a low flowable property (Madandoust et al., 2015); this can be solved by adding a Suplasticizer or Viscocrete in certain doses to improve workability.

Kodur (2014) explains that concrete material will experience quality degradation if burned at a high temperature. This can be seen from the existence of cracks and spalling in the concrete that

*Corresponding author's email: antonius@unissula.ac.id, Tel. +62-24-6583584, Fax. +62-24-6582455
Permalink/DOI: <https://doi.org/10.14716/ijtech.v10i2.2097>

are easy to occur, which will consequently cause the effect of plastic deformation of the steel reinforcement, which will trigger the loss of structural capacity. Moreover, Raouffard & Nishiyama (2016) found that the loss of load bearing capacity and the stiffness of normal concrete beams were 30% and 50%, respectively when exposed to fire. Evaluation of steel fiber-reinforced concrete material at high temperatures was conducted by Antonius et al. (2014). In order to develop a research database of fire-resistant steel fibrous concrete, various researches of steel fiber-reinforced concrete burned at a temperature of 800°C have been conducted (Shaikh & Taweel, 2015; Petrus et al., 2016). The results of this study essentially revealed that steel fiber in concrete content at a high temperature was relatively effective in reducing plastic shrinkage and spalling. Harshavardhan & BalaMurugan (2016) attempted to apply fibrous concrete to the structure of a nuclear building by making steel-fiber concrete with a high density. The constitutive equation of steel fibrous concrete at high temperatures has also been proposed by Blesak et al. (2016). Furthermore, in the field of confined steel fibrous concrete, Zaidi et al. (2016) also proposed a model of confinement of the material in the post-burn phase.

In brief, based on the research development described above, further research into the structural element of steel fibrous concrete is an interesting field of study; that is, the element of the fire resistance of the fiber reinforced concrete beam structure element up to 900°C. It is very important to experimentally study the behavior of the flexure and ductility of the beam, as this will provide more complete beam performance information from normal to high temperatures. Compared to normal concrete, which has gone through advanced research development and has been thoroughly explored (Jang et al., 2009; Antonius et al., 2017), research on reinforced fiber concrete, or more specifically reinforced concrete beams at normal to high temperatures ($\pm 900^\circ\text{C}$) given a pure bending load is still rare.

This study was conducted with the main objective of comprehensively understanding the behavior of the flexure and ductility of steel fiber reinforced concrete in normal to high temperatures. The experimental program was conducted by making a beam, with the parameters reviewed including temperature (normal temperature, 300°C, 600°C and 900°C) and the longitudinal reinforcement effect (with and without compressive reinforcement in the flexural region). The steel fiber used was limited to 0.5% of the volume of concrete. The load applied to the beam was pure bending. The research is very useful as a basis for modeling the behavior of the bending and ductility of steel fiber reinforced concrete beams. Based on the results of the study, prediction of the effect of fire incidents on the behavior of steel fibrous concrete structures can be made. In addition, the results of the study are also expected to contribute to the development of design standards, such as the Indonesian National Standard (2013) for concrete structures.

2. EXPERIMENTAL METHODS

2.1. Specimens

The concrete mix design refers to SNI 7656:2012, in which the addition of steel fiber is in the proportion of 0.5% fiber to concrete volume. The steel fiber used had a ratio of length to diameter of between 40 and 50 (Figure 1). The design of the fibrous concrete mixture can be seen on Table 1. According to ASTM C 39-94, a cylinder (150 mm in diameter and 300 mm in height) was tested for 28 days. The manufacture of the beam specimens involved two types of steel-reinforced concrete beams, without the use of compressive reinforcement in the test area (SFRC-SR), and Double Reinforcement (DR) reinforcing beams in the test area (SFRC-DR) (Antonius et al., 2013).



Figure 1 Steel fiber

Table 1 Mix design

Material	Quantity
Cement	420 kg/m ³
Fly Ash	74.11 kg/m ³
Water	160 lt/m ³
w/c	0.38
Viscocrete	6.23 lt/m ³
Sand	697 kg/m ³
Coarse aggregate	1045 kg/m ³

The dimension of the beam was 100×200×1800 mm, a size designed to match the space and loading capacity of the frame to be used. Each type of specimen consisted of four beams, with the first beam controlled or unburned, and the second, third and fourth beams burned at 300°C, 600°C and 900°C, respectively. The diameter of the longitudinal reinforcement of the beam was 10 mm (deform), with a yield stress of 582 MPa. The stirrup used 6 mm diameter plain steel. The concrete cover of all the beams was equal to 25 mm. The dimensions of the beam and details of the reinforcement are shown in Figures 2 and 3.

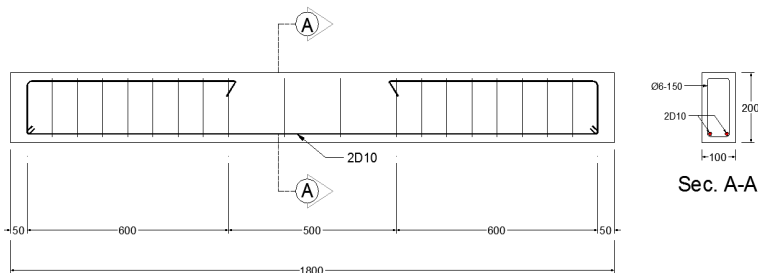


Figure 2 Beam with Single Reinforcement(SFRC-SR)

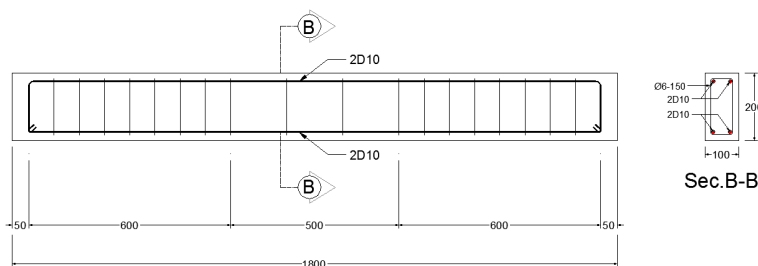


Figure 3 Beam with Double Reinforcement (SFRC-DR)

2.2. Burning of the Test Objects

In the combustion process in the combustion chamber, the temperature could be observed by a thermocouple a-mounted temperature gauge. The thermocouple was placed immediately in front of the blasting fire from the blower. In the absence of combustion, temperature readings were made using a multimeter. In the multimeter, a reading of 38.8 meant that the temperature inside the combustion chamber prior to combustion was around 38°C. Figure 4 shows the specimen burning process. Based on the temperature test in the combustion process, there is a relationship between the length of time required to reach the temperature and the combustion temperature. The relationship between the time and combustion temperature can be seen in Figure 5.



Figure 4 Specimen of burning process

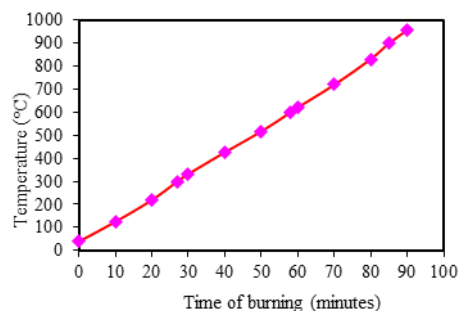


Figure 5 Relationship between time of combustion and temperature

2.3. Instrumentation and Set-up Testing

Siregar (2017) conducted concrete beam tests with a three-point loading system so that the shear effect on the beam could not be ignored. In this research, the pure flexural test of the beam employed a four-point load system, in which the test system was displacement control. The beam testing area was a pure bending area at the center of the 500 mm length, with the remainder being on the left and right-hand sides of the test region of respectively 650 mm. Support at the ends of the beam was conditioned in such a way that each support served as a joint and a roller. Figure 6 shows the loading and installation scheme of test instrumentation on the beam. A hydraulic jack, which served to continue the pressure of the hydraulic pump, was mounted vertically on the beam above the loading frame. Under the hydraulic jack, a load cell with a capacity of 200 kN was mounted for loading. To divide the load received by the beam, the load from the load cell was continued by the WF profile installed below it. Below the WF profile, two 50 mm rods were installed separate from each other, hence the loading became two points. For the beam deflection readings, an LVDT was installed under the beam, placed in the middle of the span, and on its right or left as a control. Cables from the load cell were then connected to Data Logger to record the test data.

2.4. Ductility measurement

The tests on the beams resulted in load data and beam deflection. The recorded load data were processed into the magnitude of the moment, hence we can illustrate the curve of the relationship between the moments of the beam deflection in the middle of the span. In this paper, the ductility of the beam (μ) is defined in the equation below (see Figure 7).

$$\mu = \frac{\Delta_u}{\Delta_y} \tag{1}$$

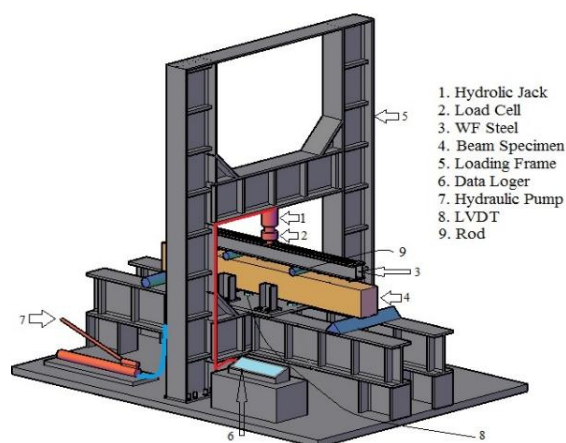


Figure 6 Testing scheme of the pure bending on the beam

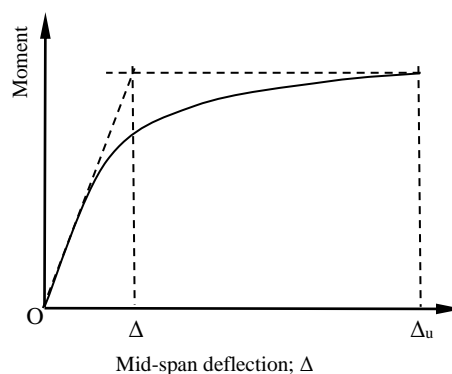


Figure 7 Ductility measurement

3. RESULTS AND DISCUSSION

3.1. Failure Pattern

The condition of the collapse of the beam against the resilient load is shown in Tables 2 and 3. Unlike the regular ash-like control beam (not burned), the burned beam at 300°C, 600°C and 900°C had a charred color, but did not show any significant spall of the fibrous concrete surface. The overall collapse pattern of the beam specimen corresponded to the usual bending theory; for example, it suffered a cracked prefix in the center zone of the span. The collapse mode applies to non-resilient beams (SR) as well as to bending reinforcement (DR). If the load continues to increase, then the crack propagation will develop slowly, accompanied by the addition of a beam deflection. The increase in the flexural load on the beam continues until the load-deflection graph on the reading exceeds the comparable limit, and the beam continues to experience a slight additional load, but the deflection increases significantly. This behavior shows excellent ductility of the beam. It can be said that at the maximum load the beam suffered a flexible collapse, and there is no indication of the existence of a sloping crack leading to the pedestal, or of crushing on the concrete. This shows the role of excellent steel fibers in maintaining the ductility of the beam.

Table 2 Failure pattern of SFRC with Single Reinforcement (SR)

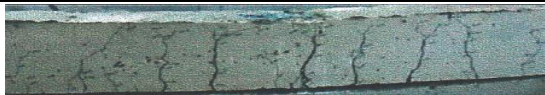
Specimen	Temperature	Single Reinforcement
SR38	Normal (38°C)	
SR300	300°C	
SR600	600°C	
SR900	900°C	

Table 3 Failure pattern of SFRC with Double Reinforcement (DR)

Specimen	Temperature	Double Reinforcement
DR 38	Normal (38°C)	
DR300	300°C	
DR600	600°C	
DR900	900°C	

3.2. Stress Degradation of Materials and Reinforcement at Elevated Temperatures

The results of the test data, including the moment and ductility of the beams, are shown in Table 4. The result of the cylindrical concrete test strength of 150×300 mm at normal temperature is 55.9 MPa. The compressive strengths of the cylindrical concrete at temperatures of 300°C, 600°C and 900°C are 38.1, 28.4 and 23.8 MPa, respectively. The percentage decrease of compressive strength to cylinder compressive strength at normal

temperature is 31.8%, 49.2% and 57.4% (see Figure 8). The results also show that starting at 600°C, the compressive strength of the cylindrical concrete has been reduced to about half of that before being burned.

Table 4 Results of Moment and Ductility

Specimen	f'_c (MPa)	SFRC-SR		SFRC-DR	
		Moment (kN-m)	Ductility (μ)	Moment (kN-m)	Ductility (μ)
T=38°C	55.9	13.56	10.3	14.19	10.9
T=300°C	38.1	12.23	6.7	13.32	10.3
T=600°C	28.4	11.13	5.1	12.98	10
T=900°C	23.8	10.05	5.1	11.94	5.3

The condition of the reinforcing steel after the beam was burnt at normal to high temperature indicates a non-significant decreasing trend in yield stress, as shown in Figure 8. The degradation of the yield stress of the reinforcing steels at 300°C, 600°C and 900°C was respectively only 14%, 16% and 17% of the yield stress of steel at normal temperatures. These values also indicate that the reinforcing steel is adequately shielded at high temperatures and still works well in its role in resisting bending of the beam. Furthermore, based on Figure 8, the best curve-fit relationship between the yield stress of the longitudinal reinforcement embedded within the fiber-reinforced beam and temperature can be described as follows:

$$f_{y(T)} = 724.9T^{-0.062} \tag{2}$$

3.3. Moments and Ductility

As shown in Table 4, the moment and ductility occurring on the beam also show a decreasing trend with increasing temperature. In contrast to the decreasing trend of the capacity of concrete cylinders in relation to the increase in the temperature imposed on the beam, the decrease of moment at high temperatures to moment at normal temperature on the SR and DR beams is not significant. Based on Table 4, at the highest temperature (900°C) the SR beam decreased by about 25% and the DR beam only decreased by about 15%. This phenomenon indicates that the loss of strength in the material due to the increase in temperature is not proportional to the behavior of the structure (in this case the beam). The loss of flexural capacity in the beam (SFRC-SR and SFRC-DR) is lower when compared to the degradation of its material strength under increasing temperature conditions (Figure 9). It is also possible from longitudinal reinforcement stresses at high temperatures that are still stable or such a stress normally used under normal temperature conditions ($f_y > 400$ MPa).

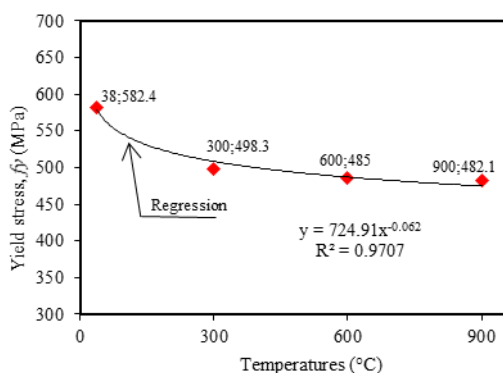


Figure 8 Average Yield Stress of Longitudinal Reinforcement at Elevated Temperatures

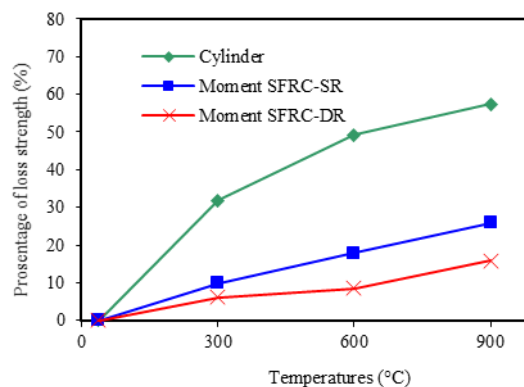


Figure 9 Loss strength of cylinder and beams

Degradation of beam ductility from normal temperature to high temperature showed significantly different values between the SR and DR specimens. As shown in Table 4 (SR specimens), ductility decreased significantly from 10.3 (at normal temperature) to 6.7 (at a temperature of 300°C). Then at 600°C and 900°C, the ductility of the beam decreased again, but not as much (to 5.1). Another phenomenon occurred in the DR specimen, from normal temperature ($\mu = 10.9$) to temperatures of 300°C and 600°C, with the ductility value decreasing, but not significantly. The decrease in ductility occurred significantly when the specimens were burned at a temperature of 900°C ($\mu = 5.3$). The difference of ductility degradation between the SR specimens and the DR ones shows that the compression reinforcement on the latter plays a good role in maintaining the ductility of the beam.

3.4. Moment-Deflection Behavior

Behavior of moment versus beam deflection in the middle of the span on the specimen shows a consistently decreasing trend when the temperature rises. This behavior applies to both the SR and DR specimens (Figures 10 and 11). At the beginning of loading, all the specimens show relatively similar behavior to each other. This begins to deviate from the linear state after the stretch of fibrous concrete extends beyond its ultimate strain and does not work; as a result, the flexural capacity of the beam depends on the longitudinal reinforcement stress. In this case, longitudinal bars can develop their tensile stress optimally and the beam deflection is greater or more ductile. Moreover, the data from the longitudinal tensile test results show an average yield stress above 400 MPa, even though the beam was burned at high temperature. In general, the ductile nature of the specimen is characterized by a longer deflection curve and tends to increase. Just as in normal concrete, compressive reinforcement in steel- fibrous concrete also plays a significant role in increasing the ductility of the beam. This is shown by the comparison between the SR and DR specimens at various temperatures (Figure 12).

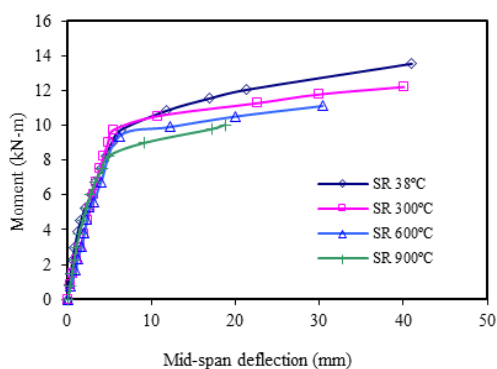


Figure 10 Moment versus mid-span deflection of the SFRC-SR specimens

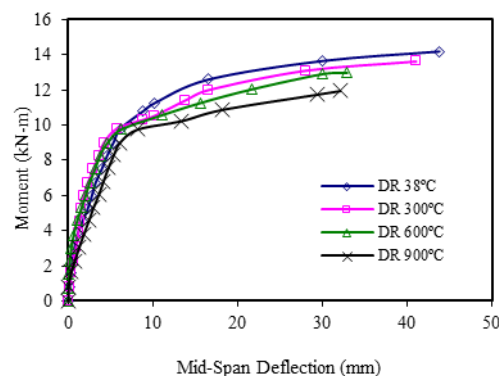


Figure 11 Moment versus mid-span deflection of the SFRC-DR specimens

4. PREDICTION OF FLEXURAL CAPACITIES FOR SFRC BEAMS AT ELEVATED TEMPERATURES

As we know, the value for concrete compressive strength testing of cylinders at normal temperature is 55.9 MPa. The moment capacity of all beams from the experimental results above can be predicted based on bending theory. The analysis of the moment capacity of the steel fiber-reinforced concrete (SFRC) beam at various temperatures is based on the calculation of the design parameters for bending (k_3 and β_1) (Harprastanti, 2017). The stress-strain model at elevated temperatures of steel-fiber concrete uses the model proposed by Antonius et al. (2014). The values of k_3 and β_1 at elevated temperatures are shown in Table 5.

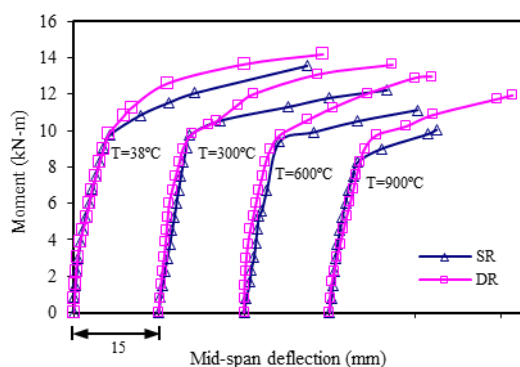


Figure 12 Comparison of SFRC beams with single and double reinforcement

Table 5 k_3 and β_1 values

Temperature (°C)	k_3	β_1
38	0.97	0.75
300	0.92	0.75
600	0.92	0.75
900	0.92	0.75

Based on the values of k_3 and β_1 for steel-fiber concrete at 38°C, 300°C, 600°C, and 900°C being obtained and longitudinal reinforcement at various temperatures using Equation 2. A comparison of the theoretical and experimental results is shown on Table 6. Overall, the moment values of the analysis results and the experimental results do not differ significantly.

Table 6 Moment of analytical and experimental results

Specimen	Moment (kN-m)		$M_{analytical}/M_{exp.}$
	Analytical	Exp.	
SR38	15.67	13.56	1.15
SR300	13.41	12.23	1.10
SR600	12.08	11.13	1.09
SR900	11.41	10.05	1.14
DR32	15.64	14.19	1.10
DR300	13.39	13.32	1.00
DR600	12.56	12.98	0.97
DR900	12.35	11.94	1.03

5. CONCLUSION

The specimens of steel fiber reinforced concrete beams behave purely and did not experience shear failure. This shows the role of steel fibers in developing significant flexural deformations. The collapse pattern applies to both single-reinforcement system specimens and double reinforcement systems. The higher the temperature, the lower the decrease in the flexural beam capacity of the double reinforcement system than that of the single-beam reinforcement density system. Compared with the moment in each type of beam, the percentage of loss of flexural capacity of the beam without compressive pressure is higher. The beam without compressive reinforcement lost its ductility faster, by almost 50% (from normal temperature to a temperature of 300°C). But the ductility degradation of the beam with the compressive reinforcement was not significant (from normal up to a temperature of 600°C). The longitudinal reinforcement embedded in the steel fibrous concrete was highly protected against high temperatures, whereas

the initial yield stress only lost a maximum of 17% of the yield stress at 900°C. The prediction of flexural capacity using a constitutive model of steel fibrous concrete at various temperatures is very good and relatively close to the experimental flexural capacity.

6. ACKNOWLEDGEMENT

The experimental program presented in this paper is the second year of the results of the Competitive Research Program (*Hibah Bersaing*), Contract No. 002/006.2/PP/SP/2013, funded by the Directorate General of Higher Education, Ministry of Education and Culture, Republic of Indonesia, and conducted at the Structural Laboratory, Department of Civil Engineering, Semarang State University. The support received for this research is gratefully acknowledged.

7. REFERENCES

- Antonius, 2015. Strength and Energy Absorption of High-strength Steel Fiber Concrete Confined by Circular Hoops. *International Journal of Technology*, Volume 6(2), pp. 217–226
- Antonius, Widhianto, A., Darmayadi, D., Asfari, G.D., 2014. Fire Resistance of Normal and High-strength Concrete with Contains of Steel Fibre. *Asian Journal of Civil Engineering*, Volume 15(5), pp. 655–669
- Antonius, Imran, I., Setiyawan, P., 2017. On the Confined High-strength Concrete and Need of Future Research. *Procedia Engineering*, Volume 171, pp. 121–130
- Antonius, Darmayadi, D., Asfari, G.D., 2013. *Mechanical Properties of Steel Fiber Concrete at High Temperatures*. Competitive Research Report, Directorate General of Higher Education [in Indonesian]
- ASTM C 39–94, 1996. *Test Method for Compressive Strength of Cylindrical Concrete Specimens*. Annual Books of ASTM Standards. USA
- Blesak, L., Goremikins, V., Wald, F., Sajdlova, T., 2016. Constitutive Model of Steel Fibre Reinforced Concrete Subjected to High Temperatures. *Acta Polytechnica*, Volume 56(6), pp. 417–424
- Dhinakaran, G., Vijayarakhavan, S., Kumar, K.R. 2016. Fracture and Flexural Behavior of High-performance Fiber Reinforced Concrete. *Asian Journal of Civil Engineering*, Volume 17(1), pp. 1–14
- Han, A.L., Antonius, Okiyarta, A.W., 2015. Experimental Study of Steel Fiber Reinforced Concrete Beams with Confinement. *Procedia Engineering*, Volume 125, pp. 1030–1035
- Harprastanti, P., 2017. *Flexural Behavior of Steel Fiber Reinforced Concrete Beams at Post Burning*. Master Thesis, Graduate Program, Diponegoro University, Indonesia [in Indonesian]
- Harshavardhan, C., BalaMurugan, S., 2016. Study on High-density Concrete Reinforced with Steel Fiber at Elevated Temperatures. *ARNP Journal of Engineering and Applied Sciences*, Volume 11(19), pp. 11415–11420
- Indonesian National Standard, SNI 2847-2013. *Requirements of Structural Concrete for Building* [in Indonesian]
- Indonesian National Standard, SNI 7656:2012. *Procedures of Mixed Selection for Normal Concrete, Heavy Concrete and Mass Concrete* [in Indonesian]
- Iqbal, S.A., Ali, K., Holschemacher, Bier, T.A., 2015. Mechanical Properties of Steel Fiber Reinforced High Strength Lightweight Self-Compacting Concrete (SHLSCC). *Construction and Building Materials*, Volume 98, pp. 325–333
- Janani, S., Santhi, A.S., 2018. Multiple Linear Regression Model for Mechanical Properties and Impact Resistance of Concrete with Fly Ash and Hooked-end Steel Fibers. *International Journal of Technology*, Volume 9(3), pp. 526–536

- Jang, I-Y., Park, H-G., Kim, Y-G., Kim, S-S., Kim, J-H., 2009. Flexural Behavior of High-strength Concrete Beams Confined with Stirrups in Pure Bending Zone. *International Journal of Concrete Structures and Materials*, Volume 3(1), pp. 39–45
- Jansson, A., Lofgren, I., Lundgren, K., Gyltoft, K., 2012. Bond of Reinforcement in Self-compacting Steel-fibre-reinforcement Concrete. *Magazine of Concrete Research*, Volume 64(7), pp. 617–630
- Kodur, V., 2014. Properties of Concrete at Elevated Temperatures. *ISRN Civil Engineering*, Volume 2014, ID 478510
- Madandoust, R., Ranjbar, M.M., Moshiri, A.A., 2015. The Effect of Steel and Pet Fibers on the Properties of Fresh and Hardened Self-compacting Concrete. *Asian Journal of Civil Engineering*, Volume 16(7), pp. 955–966
- Petrus, C., Azhar, H.A., Dee, G.L., Ismail, R., Alisibramulisi, A., 2016. Compressive Strength of Concrete with Fibres at Elevated Temperatures. *Jurnal Teknologi*, Volume 78(4), pp. 71–74
- Raouffard, M.M., Nishiyama, M., 2016. Residual Load Bearing Capacity of Reinforced Concrete Frames After Fire. *Journal of Advanced Concrete Technology*, Volume 14(10), pp. 625–633
- Shaikh, F.U.A., Taweel, M., 2015. Compressive Strength and Failure Behaviour of Fibre Reinforced Concrete at Elevated Temperatures. *Advances in Concrete Construction*, Volume 3(4), pp. 283–293
- Siregar, A.P.N., 2017. Measuring the Effect of Strengthened Concrete on the Fracture Characteristics of Notched Concrete Beams Through a Three-point Beam Test. *International Journal of Technology*, Volume 8(4), pp. 737–746
- Zaidi, K.A., Sharma, U.K., Bhandari, N.M., Bhargava, P., 2016. Post Heated Model of Confined High Strength Fibrous Concrete. *Advances in Civil Engineering*, Article ID 5659817